Delineation of Region of Interest Volume in Cardiac Gated PET Images

J Gubbi[1], M Palaniswami[1], K Tomas[2], D Binns[2], M Griffiths[3]

[1]The University of Melbourne, Melbourne, Australia
[2]Peter MacCallum Cancer Institute, Melbourne, Australia
[3]Royal Brisbane Hospital, Brisbane, Australia

Abstract

Positron Emission Tomography is a state of art functional imaging technique used in accurate detection of cancer. Regions of interest including tumor in the thoracic region face a unique problem of movement due to the involuntary motion of the organs. To avoid irradiation of healthy tissues during radiotherapy treatment planning, accurate tracking of the moving parts during different stages of cardiac cycle is recommended. Cardiac gating is a process of dividing a single cardiac cycle into several phases and sorting the data into each of these phases according to the location of the acquired image. The aim of this study is to accurately track the movement in cardiac gated PET images. The proposed method is a two stage approach with an initial preprocessing stage and level set deformable model is used in the second stage. The proposed method is tested on six patients' cardiac gated data resulting in accuracies ranging between 87% and 94% in terms of percentage volume overlap.

1. Introduction

Lung carcinoma is caused by the uncontrolled growth and division of cells in the lungs. According to a 2008 survey from the American Cancer Society (www.cancer.org), lung cancer afflicts about 3 million people, and is a major cause of death in the developing world. A recent article on an Australian government web-site (Health In-site, www.healthinsite.gov.au) indicates that lung cancer is the leading cause of death in Australia killing about 7000 people every year. Only one in ten patients diagnosed with lung cancer will survive the next five years.

Positron emission tomography is a powerful and versatile imaging tool for detecting lung cancer. It offers a unique opportunity to visualize and measure the pathophysiology and key biological parameters that influence the disease diagnosis, development and outcome. In general, PET scans measure important body functions, such as blood flow, oxygen use and glucose metabolism to evaluate how well organs and tissues are functioning.

Gating is a technique that reduces the smearing effect on the images by providing clearer and improved visualizations of tumors during respiration. In order to correct the lung motion and heart motion on the images, PET data is divided into small parts with each part representing only a fraction of the total motion based on either respiratory cycle or cardiac cycle. This division is called gating and are called respiratory gating and cardiac gating respectively. Accuracy in delineating the volume of the region of interest is extremely important for proper radiotherapy treatment planning. The definition of target or tumor volumes in lung cancer by the treating physician has been found to bear the largest source of error in the whole chain of radiotherapy [1] treatment. With each breath or heart beat, organs in the chest and abdomen move. As the lungs expand and contract while inhaling and exhaling, lung tumors move within a 2-inch range and may even change shape, making precise targeting of radiation beams difficult. When treating the tumor with external radiation, the physicians include certain extra margin (up to 2.5 cm.) of healthy tissues surrounding the detected tumor volume for radiation, to cater for tumor movement during respiration. Hence thoracic motion often results in overestimation of the volume of the lung lesions, which in turn results in destroying more healthy tissues around the tumor.

We have dealt with automatic tumor volume delineation using respiratory gating elsewhere [2] and will concentrate on cardiac gating in this work. In cardiac gating of the normal heart rhythm of the patient is divided into eight parts by using the cardiac cycle. The PET list-mode (event by event) data is sorted into these eight gates in accordance with the phase of cardiac signal, thus resulting in eight image sets with reduced motion [3]. Compared to our earlier work [2], the following improvements are made apart from using cardiac gated images (a) the type of images considered are much more noisier with different types of noise (b) the machine learning step proposed earlier is completely

bypassed as this introduced lot of false alarms due to the presence of noise. Moreover, in cardiac gated images both tumor and the other regions of interest such as the heart is tracked simultaneously. To achieve this, a preprocessing step based on the standard uptake value (SUV) is performed followed by level set deformable model for tumor tracking.

2. Methods

In this section, brief description of the data, preprocessing using standard uptake value and level set method is presented. The data was collected from two separate sources in Melbourne and Brisbane in Australia between 2006 and 2008. Totally six patient datasets are used in the analysis of the proposed method. A brief summary of the data is given in table 1. It should be noted that due to lack of availability of data, only one data with tumor was available and all other datasets had heart movement which is used in the region of interest tracking.

2.1. Preprocessing using SUV

Standardized uptake value [4] is the most commonly used parameter in clinical practice to quantify the intensity of radio tracer F-18-fluoro-deoxy-glucose (FDG) uptake in tumors. This has been used as an index of glucose metabolism to classify malignant tumors based on the amount of uptake in the given region of interest in relation to the average uptake throughout the body. Tumor cells metabolize more glucose than normal or healthy cells. Hence, in general, if the tumor is present it appears brighter than healthy cells in a PET image. Calculation of SUV [5] is the most common way to compare the regions of interest between different patients. For each voxel, assuming $1cc = 1g$ SUV is calculated by applying equation $SUV = \frac{YW}{D}$, where Y is the activity concentration in Bq/cc, W is the patient weight in kilograms (kg) and D is the injected dose at the start of the scan expressed as Becquerel (Bq). Tissue activity concentration Y is calculated using the formula $Y = ax + b$, where x is the original pixel intensity value, a is the rescale slope and b is the rescale intercept for each image slice of the PET scan. With this definition, if the injected dose were uniformly distributed over the entire body, then the SUV values everywhere would be approximately equal to 1. In general the higher the SUV value, the more aggressive is the tissue activity which applies for both heart and tumor in the thoracic region. Most investigators choose an SUV threshold of 2.5 to differentiate benignity from malignancy in lung lesions [6]. SUV runs into controversy [7] in defining this threshold value because of the various physical parameters like patient weight, glucose level, length of the uptake period and body composition that are involved for this value calculation. In this work, after analyzing the data a SUV threshold of 2 is chosen. If the SUV value is greater than or equal to 2.0, the pixel is taken as the foreground; otherwise, it is taken as background. Because of noise in the image, accurate final segmentation cannot be accomplished with this step. However, there is huge reduction in noise by using this step for pre processing.

Patient ID	Number of 2D images	Slices per frame	Nature of the dataset
P1	376	47	Clean, Tumor and Heart
B1	360	45	Noisy, Heart
B2	280	35	Noisy, Heart
B3	288	36	Clean, Heart
B4	336	42	Noisy, Heart
B5	360	45	Very Noisy, Heart

Table 1. Summary of the data used in this study. All patients had 8 frames of data.

2.2. Level set deformable models

A deformable model was introduced by Kass *et al.* [8] in 2D as explicit deformable contours and this was generalized to 3D by Terzopoulos *et al.* [9]. Deformable model are curves or surfaces defined within an image domain. By incorporating other prior information about the object shape, these models offer robustness to both image noise and boundary gaps. In the level set method [10], the model M is implicitly defined as the zero level set of a higher dimension function v. Starting from a given shape M_0, the model is able to evolve towards the shape of the object, according to the first-order evolution law given in equation 1

$$\frac{\partial M}{\partial t} = F\vec{N} = (F_{int} + F_{ext})\vec{N} \tag{1}$$

with F representing the force applied on the surface and the surface normal vector $\vec{N}$. This force F is decomposed into internal component F_{int} and external component F_{ext}. Given an initial surface M_0, the level set function is $v(x, y) = d((x, y), M_0)$ where d is a signed distance. The initial contour is defined as $M = (x, y)|v(x, y) = 0$. v is represented as a distance map. The map values outside the contour are positive while inside they are negative [11]. The level set method shows that the model evolution shown in equation 1 corresponds to an evolution of the distance map satisfying the equation 2

$$\frac{\partial v}{\partial t} = F\|\nabla v\| = (F_{int} + F_{ext})\|\nabla v\| \tag{2}$$

where $v(x, y, t)$ is the evolutive distance map. Equation 2 is only valid at the model location. As a consequence, the distance map of v will not be preserved. In order to cope with this problem there is a need to re-initialize v periodically so that it corresponds to a distance map. Unfortunately, there are many drawbacks associated with re-

initialization. A new variational formulation for geometric active contours which completely eliminates the need of the costly re-initialization procedure has been proposed by Chunming *et al.* [12] and is used in this work. Their variational formulation consists of an internal energy term that penalizes the deviation of the level set function from a signed distance function, and an external energy term that drives the motion of the zero level set toward the desired image features, such as object boundaries. The resulting evolution of the level set function is the gradient flow that minimizes the overall energy function.

In spite of using the new algorithm without re-initialization, there is another drawback with this algorithm. The initialization and the number of iterations required for accurate detection has to be manually input by trial and error. A very simple yet effective strategy to address this issue has been proposed. The first frame is subjected to normal algorithm with the entire region as the initial boundary. The number iteration is set to fairly large number and the algorithm is initiated. This is validated by the expert and the corrections to the boundary are suggested to the algorithm using a custom made GUI where the level set convergence is available for tracking the progress in the reverse direction. For subsequent frames, the small area around the region of interest detected in the first frame is used as initial contour for subsequent frames. The number of iterations is obtained from the first frame which is already validated by the expert using the reverse tracking process. This ensures that the time taken for subsequent frames is relatively lesser and the region of interest tracking is more accurate with less false alarms.

3. Results

The results are summarized in table 2. Overall percentage overlap volume between manually segmented and the automatically segmented images ranged between 87% for patient B5 to 94% for patient P1. The time taken for the first frame varied depending on the volume and took 2 minutes to 8 minutes. After expert validation, the time taken for the remaining frames including expert validation was much lesser. This is encouraging as the method not only reduces expert fatigue due to manual segmentation but also enables more consistency in segmentation between frames and subjects. As expected the noisy data of patient B5 resulted in least accuracy of 87% in terms of percentage volume overlap and took maximum amount of time to complete. The segmentation results of 6 slices from different subjects is shown in figure 1. The top three sub-figures are results of good segmentation and the bottom three show the results of average segmentation. The false alarms and the region of interest detection in the bottom row are not as accurate as the images in the top row. The middle image in the top row shows the results of patient P1 where both the heart and the tumor are detected accurately. Once we have this result for the first frame, the expert can remove heart as the region of interest and only the tumor can be tracked in the subsequent frames. However, the results calculated in this paper is for both the regions of interest.

	Frame 1		**Frames 2 - 8**		
Patient ID	Time taken (min)	EV (min)	Time taken for other frames (min)	EV (min)	ROI volume overlap %
P1	4	20	20	30	94
B1	5	25	15	45	91
B2	3	15	16	30	89
B3	2	16	11	42	90
B4	4	25	19	35	89
B5	8	30	23	76	87

Table 2. Overall results (last column) and time evaluation using the proposed method. EV - Expert Validation (approximate time); ROI - Region of Interest

4. Conclusions

Positron Emission Tomography plays a major role in detecting cancer in thoracic regions which is one of the most lethal of cancers worldwide. To avoid irradiation of healthy tissues during radiotherapy treatment planning, accurate tracking of region of interest including tumor during different stages of respiratory or cardiac cycle is recommended. Currently manual segmentation is used for radiotherapy treatment planning which is tedious and inconsistent. The aim of this study is to accurately track the movement of the regions of interest specifically tumor in cardiac gated PET images. The proposed method uses SUV based pre-processing followed by a two stage tracking using deformable models. The method is tested on six patients' cardiac gated dataset with percentage volume overlap in the range of 87% and 94%. The overall time taken is much lesser than manual segmentation including expert validation. Thus, the level set accurately delineated the tumor volume from all eight frames, thereby, providing a scope of using PET images towards planning an accurate and effective radiotherapy treatment for thoracic cancer.

References

[1] Rasch C, Remeijer P, Koper P, Meijer G, Stroom J, van Herk M, Lebesque J. Comparision of Prostate Cancer Treatment in two Institutions: A Quality Control Study. International Journal of Radiation Oncology 1999;45:1055–1062.

[2] Kanakatte A, Gubbi J, Srinivasan B, Mani N, Tomas K, Binns D, Palaniswami M. Pulmonary Tumor Volume Delineation in PET Images using Deformable Models. In Proceedings of the 30th Annual International Conference of the

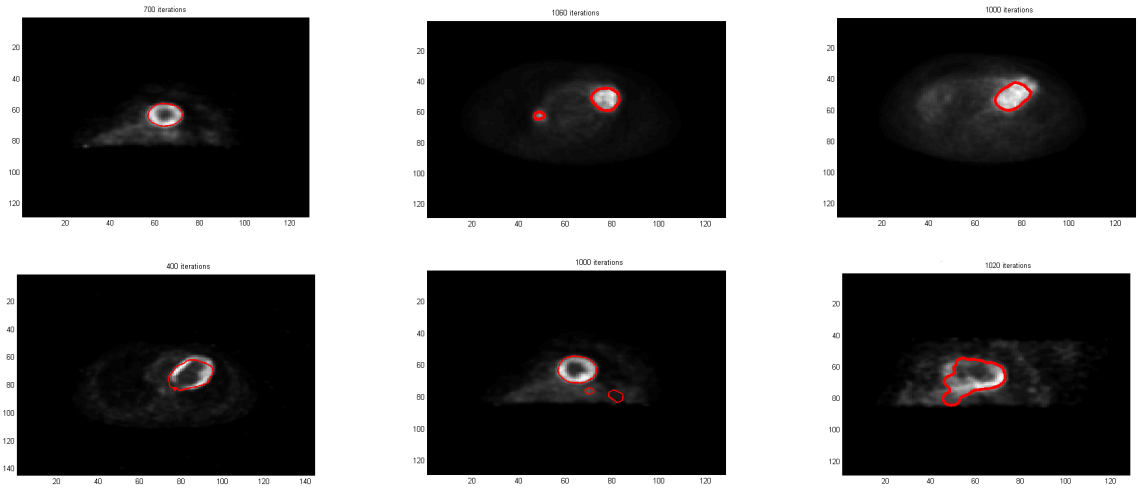

Figure 1. Result of region of interest tracking in frames 2 to 8. Top three images show good segmentation and the bottom three show average segmentation. Middle column top image shows correct tumor and heart segmentation and middle column bottom figure shows false alarms

IEEE Engineering in Medicine and Biology Society (IEEE EMBC'08). IEEE Press, 2008; 3118–3121.

[3] Dawood M, Lang N, Jiang X, Schafers K. Lung motion correction on respiratory gated 3d pet/ct images. IEEE Transactions on Medical Imaging 2006;25(4):476–485.

[4] Thie J. Understanding the standardised uptake value, its methods and implications for usage. The Journal of Nuclear medicine 2004;45(9):1431 – 1434.

[5] Jakobsson D, Olofsson F. Decision Support System for Lung Cancer using PET/CT Images. Lund University of Technology, 2004.

[6] Matthies A, Hickeson M, Cuchiara A, Alavi A. Dual time point 18f-fdg pet for evaluation of pulmonary nodules. Nuclear Medicine 2002;43(7):871–875.

[7] Keyes Jr J. SUV: Standard Uptake or Silly Useless Value. Nuclear Medicine 1995;36(10):1836–1839.

[8] Kass M, Witkin A, Terzopoulos D. Snakes: Active contour models. International Journal of Computer Vision 1988; 1:321–331.

[9] Terzopoulos D, Witkin A, Kass M. Constraints on deformable models: Recovering 3d shape and nonrigid motion. Journal of Artificial Intelligence 1988;36(1):91–123.

[10] Osher S, Sethian A. Fronts Propagating with Curvature Dependent Speed: Algorithms based on Hamilton - Jacobi Formulations. Journal of Computational Physics 1988; 79:12–49.

[11] Charnoz A, Lingrand D, Montagnat J. A Levelset Based Method for Segmenting the Heart in 3D+T Gated SPECT Images. In Proceedings of Functional Image and Modeling of the Heart Conference. 2003; 52–61.

[12] Li C, Xu C, Gui C, Fox M. Level set Evolution without Re-initialization: A New Variational Formulation. In Proceedings of IEEE CVPR Conference. 2005; 430–436.

Address for correspondence:

A/Prof. M. Palaniswami
ISSNIP, Dept of Electrical and Electronic Engineering
The University of Melbourne, Vic - 3010, Australia.
palani@unimelb.edu.au